Nonuniformly Spaced Photonic Microwave Delay-Line Filters and Applications

Yitang Dai and Jianping Yao, *Senior Member, IEEE*

***Abstract*—A finite impulse response (FIR) filter for microwave signal processing implemented based on an optical delay-line structure with uniformly spaced taps has been extensively investigated, but the realization of such a filter with negative or complex tap coefficients to provide an arbitrary frequency response is still a challenge. In this paper, an overview of photonic microwave delay-line filters with nonuniformly spaced taps, by which an arbitrary bandpass frequency response can be achieved with all-positive tap coefficients, is presented. We show that the nonuniform time delays provide equivalent phase shifts to the tap coefficients, while the all-positive-coefficient nature simplifies greatly the filter realization. Based on the theory, a 50-tap flat-top bandpass filter with a quadratic phase response is designed and analyzed. A seven-tap nonuniformly spaced photonic microwave filter with a flat-top and chirp-free bandpass response is then demonstrated. The use of the proposed technique for advanced microwave signal processing is then discussed. The generation of a chirped microwave signal and a phase-coded microwave signal are discussed and demonstrated. The use of the proposed technique to design a FIR filter for microwave matched filtering is also discussed and experimentally demonstrated.**

***Index Terms*—Finite impulse response (FIR), microwave photonics, nonuniformly spaced sampling, optical processing of microwave signals.**

I. Introduction

PROCESSING OF microwave signals in the optical domain has been a topic of interest for many years [1], [2]. The key advantage of using photonics techniques is the high speed, which overcomes the inherent bottleneck caused by the limited sampling rate of currently available digital electronics. In addition, a photonic microwave signal processor provides other advantages such as large tunability and reconfigurability, low loss, light weight, and immunity to electromagnetic interference [1], [2]. Among the many processor configurations, the one with a finite impulse response (FIR) is the most popular configuration thanks to the simplicity and implementability in the optical domain, which has been pursued intensively in the past few years. In a FIR filter, the input signal is time delayed, weighted, and then summed as the output. To avoid optical interference, a photonic microwave FIR filter is usually designed to operate in the incoherent regime, which leads to all-positive coefficients or special designs have to be incorporated to generate negative or complex coefficients. It is known that a FIR filter with all positive coefficients can provide very limited functionalities. In practice, it is often desired that the filter has a bandpass response with flat top and sharp transition bands. To do so, negative or complex coefficients are required. In addition, for advanced microwave signal processing, a FIR filter with a sophisticated phase response, such as a quadratic phase response, is usually required, which leads to the requirement for negative or complex coefficients. As a result, techniques to generate negative and complex tap coefficients in a photonic microwave FIR filter are highly desirable.

Many techniques have been proposed and demonstrated to implement an incoherent photonic microwave FIR filter with negative or complex coefficients. One straightforward approach to generating negative coefficients is to perform differential detection using a balanced photodetector (PD) [3]. Other techniques to generate negative coefficients include the use of cross-gain modulation (XGM) [4] or cross polarization modulation (XPolM) [5] in a semiconductor optical amplifier (SOA), carrier depletion effect in a distributed-feedback laser diode (LD) [6] or in a Fabry–Pérot LD [7], and the use of the transmission of a broadband source through uniform fiber Bragg gratings (FBGs) [8]. Negative coefficients can also be generated by biasing a pair of Mach–Zehnder modulators (MZMs) at the opposite slopes of the transfer functions to achieve amplitude inversion [9], or by using a single dual-output MZM with a double-pass modulation [10]. Recently, we have proposed to implement a photonic microwave FIR filter with negative coefficients based on phase modulation to intensity modulation (PM-IM) conversion in an optical frequency discriminator [11], [12]. Depending on the locations of the optical carriers at the positive or negative slopes of the frequency discriminator, positive or negative coefficients are generated.

The implementation of a photonic microwave FIR filter with complex coefficients has also been recently demonstrated. In [13], a complex coefficient was generated using a system consisting of three PDs and two broadband phase-shifted microwave couplers. In [14], the system consists of two MZMs and a broadband 90° phase shifter [14]. Since electronic phase shifters were used, the above systems were not all optical, but hybrid. In [15], an all-optical approach to generating a complex coefficient was proposed. The complex coefficient was generated by changing the phase of the microwave signal realized based on a combined use of optical single-sideband modulation (SSB) and stimulated Brillouin scattering (SBS).

Based on the above overview, we may conclude that to implement a photonic microwave FIR filter with negative or com-

Manuscript received January 06, 2010; revised July 19, 2010; accepted July 29, 2010. Date of publication October 04, 2010; date of current version November 12, 2010. This work was supported by the Natural Sciences and Engineering Research Council of Canada (NSERC).

The authors are with the Microwave Photonics Research Laboratory, School of Information Technology and Engineering, University of Ottawa, Ottawa, ON, Canada K1N 6N5 (e-mail: jpyao@site.uOttawa.ca).

Color versions of one or more of the figures in this paper are available online at http://ieeexplore.ieee.org.

Digital Object Identifier 10.1109/TMTT.2010.2074570

plex coefficients, the filter should have a complicated structure, which is hard to implement, especially for a filter with a large number of taps.

Recently, we have proposed a new concept to introduce a phase shift to a microwave signal based on optical time delay by which the phase coding of a microwave pulse, which should generally be achieved by a microwave FIR filter with complex coefficients, was realized using a FIR filter having all positive coefficients, with the phase information encoded by the time delays [16]. The same concept has recently been applied to the design of a flat-top photonic microwave filter [17], to the generation of a chirped microwave pulse [18], and to the implementation of a microwave matched filtering [19]. In all the applications, the tap coefficients are kept positive only. Our demonstrations showed that the FIR filters having all-positive coefficients with nonuniformly spaced taps can achieve equivalently the functionalities that require negative or complex tap coefficients. Although the concept of the time-delay-based phase shift has been demonstrated, until now a thorough theory, to show the relationship between the nonuniform sampling and the filter spectral response, has not been established.

In this paper, an overview of photonic microwave delay-line filters with nonuniformly spaced taps, by which an arbitrary bandpass frequency response can be achieved with all-positive tap coefficients, is presented. We start with a theoretical study on the design of a nonuniformly spaced microwave FIR filter. We show that a nonuniformly spaced microwave FIR filter with all positive coefficients would function the same as a regular uniformly spaced FIR filter with true negative or complex coefficients, or more accurately, the spectral response of a specific passband of a nonuniformly spaced microwave FIR filter would be exactly identical to that of a microwave FIR filter with true negative or complex coefficients. A mathematical expression that relates the required nonuniform sampling, i.e., the time delays or equivalently the coefficients of the taps, and the required arbitrary bandpass response is developed. As a design example, a 50-tap flat-top bandpass filter with a quadratic phase response is designed. A seven-tap nonuniformly spaced photonic microwave filter with a flat-top and chirp-free bandpass response is then experimentally demonstrated [17]. The proposed technique is particularly useful for advanced microwave signal processing, such as chirped and phase-coded microwave pulse generation and microwave pulse compression, since the specific passband can be designed to be exactly identical to that of a microwave FIR filter with true negative or complex coefficients. A discussion on the use of the proposed technique for the generation of a chirped [18] and phase-coded microwave pulse [16] and for the implementation of microwave matched filtering [19] is reviewed. Experimental demonstrations are then performed.

This paper is organized as follows. In Section II, the theory of a nonuniformly spaced FIR filter is presented and an expression that relates the nonuniform sampling and the filter spectral response is established. In Section III, a design example is provided in which a 50-tap FIR filter with a flat-top passband and a quadratic phase response is designed. Some issues associated with the filter design are addressed. An experimental demonstration is then provided, in which a seven-tap FIR filter with a flat-top and chirp-free bandpass response is then implemented. In Section IV, a discussion on the use of the proposed FIR filter for advanced microwave signal processing is presented. The generation of a chirped microwave signal and a phase-coded microwave signal are discussed and demonstrated. The use of the proposed technique to design a FIR filter for microwave matched filtering is also discussed and experimentally demonstrated. In Section V, a conclusion is drawn.

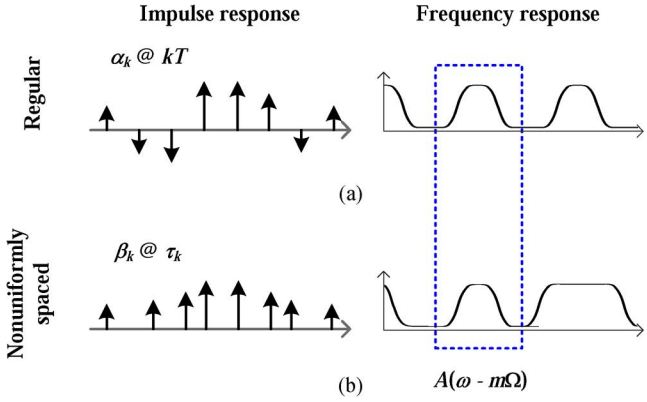

Fig. 1. Comparison between the spectral responses of a: (a) regular uniformly spaced FIR filter and (b) nonuniformly spaced FIR filter. The desired bandpass response, marked in the dotted box, can be realized in a FIR filter by nonuniform sampling with all-positive coefficients.

II. Principle

The comparison between a nonuniformly spaced FIR filter having all-positive coefficients and a regular uniformly spaced FIR filter with true negative or complex coefficients is shown in Fig. 1. It is known that a FIR filter has a multichannel frequency response with the channel spacing equal to the free spectral range (FSR) of the filter. For a regular FIR filter, all the channels have the same spectral response, as shown in Fig. 1(a). We will show that if the filter taps are nonuniformly spaced, the spectral responses of the multiple channels will be different, as shown in Fig. 1(b). By properly designing the nonuniform sampling function, we can get a spectral response at a specific bandpass that is identical to that of a regular uniformly spaced FIR filter, as shown in the dotted box in Fig. 1.

In the following, we will derive a mathematical expression that relates the nonuniform sampling function and the filter spectral response. The derivation will start with a regular FIR filter having uniformly spaced taps. Generally, the impulse response of a regular FIR filter can be expressed as

$$h(t) = \sum_{k=0}^{N-1} \alpha_k \delta(t - kT) \tag{1}$$

where N is the tap number, α_k is the tap coefficient of the kth tap, $T = 2\pi/\Omega$ is the time delay difference between two adjacent taps, and Ω is the FSR of the filter. The expression of $h(t)$ can be expressed in another form

$$h(t) = a(t)s_0(t) \tag{2}$$

where $a(t)$ is the coefficient profile, which can be complex valued

$$\alpha_k = a(kT) \text{ and } a(t) = 0 \text{ if } t < 0 \text{ or } t \geqslant NT \tag{3}$$

and $s_0(t)$ is the sampling function given by

$$s_0(t) = \sum_k \delta(t - kT). \tag{4}$$

Based on (2), the frequency response $H(\omega)$ of the regular FIR filter can be calculated by the Fourier transform

$$\begin{aligned} H(\omega) &= \frac{1}{2\pi} A(\omega) * \sum_m \Omega\delta(\omega - m\Omega) \\ &= \sum_m \frac{1}{T} A(\omega - m\Omega) \end{aligned} \tag{5}$$

where $A(\omega)$ is the Fourier transform of $a(t)$ and $*$ denotes the convolution operation. For practical applications, the FSR of the filter, Ω, should be larger than the bandwidth of $A(\omega)$. The frequency response of the regular FIR filter then has multiple channels with the spectral response of each channel being the same as $A(\omega)$, and the mth channel is located at $m\Omega$.

Based on (5), we conclude that for a regular uniformly spaced FIR filter, the tap coefficient profile is just the inverse Fourier transform of the desired bandpass response. If a FIR filter with an arbitrary bandpass response is desired, $a(t)$ should not be positive only, but negative or complex tap coefficients are required, which are determined by (3).

However, if the time-delay spacing is nonuniform, the bandpass response is no longer the Fourier transform of the tap coefficients profile. To describe the impulse response of a nonuniformly spaced FIR filter $\tilde{h}(t)$, we modify (2) by introducing a time-delay shifting function $f(t)$

$$\tilde{h}(t) = |b(t)| \times s_0[t + f(t)] \tag{6}$$

where $|b(t)|$ is a positive-only coefficient profile. Based on (4) and (6), the impulse response of the nonuniformly spaced FIR filter can also be expressed in a conventional form

$$\begin{aligned} \tilde{h}(t) &= |b(t)| \times \sum_k \delta[t + f(t) - kT] \\ &= \sum_k \beta_k \delta(t - \tau_k) \end{aligned} \tag{7}$$

where β_k and τ_k are the tap coefficient and time delay of the kth tap, respectively. From (7), we have

$$\tau_k = kT - f(\tau_k) \tag{8a}$$

$$\beta_k = \left| \frac{b(\tau_k)}{1 + f'(\tau_k)} \right| \tag{8b}$$

which shows that the proposed filter is nonuniformly spaced and has all-positive coefficients. Note that (8b) is obtained by considering the property of the Dirac function.

Although a precise close-form frequency response of the proposed FIR filter, i.e., the Fourier transform of (6), is hard to obtain, $\tilde{h}(t)$ can still be expressed as the sum of many bandpass responses with different central frequencies. Note that $s_0(t)$ can be expressed based on the Fourier series expansion

$$s_0(t) = \sum_m \frac{1}{T} \exp(jm\Omega T). \tag{9}$$

Based on (9) and (6), we have

$$\tilde{h}(t) = \sum_m \frac{1}{T} |b(t)| \exp[jm\Omega f(t)] \times \exp(jm\Omega t). \tag{10}$$

If we assume that $B_m(\omega)$ is the Fourier transform of $|b(t)| \exp[jm\Omega f(t)]$, then the frequency response of the nonuniformly spaced FIR filter is

$$\tilde{H}(\omega) = \sum_m \frac{1}{T} B_m(\omega - m\Omega). \tag{11}$$

If the FSR, Ω, is larger than the bandwidth of $B_m(\omega)$, then the proposed FIR filter would still have a multichannel frequency response. However, it is different from a regular FIR filter described by (5), as the response of each channel is not the Fourier transform of the coefficient profile and the multichannel responses are no longer identical. The bandpass frequency response $B_m(\omega - m\Omega)$ is determined by the tap coefficient profile $|b(t)|$, the nonuniform sampling function $f(t)$, and the channel order m. It should be noted that, in (10), the nonuniform sampling function $f(t)$ provides an additional phase modulation (PM) to the all-positive coefficient profile $|b(t)|$, which ensures that an arbitrary bandpass response can be realized by the proposed FIR filter with all-positive coefficients via nonuniform sampling.

Now we assume that the bandpass of interest is located at $m\Omega$ with a frequency response given by $(1/T)A(\omega - m\Omega)$. Based on (11), one can then get

$$\frac{1}{T} B_m(\omega - m\Omega) = \frac{1}{T} A(\omega - m\Omega) \tag{12}$$

which means that the desired bandpass response will be achieved in the mth channel of the proposed nonuniformly spaced FIR filter. By applying the inverse Fourier transform to (12), we have

$$|b(t)| \exp[jm\Omega f(t)] = |a(t)| \exp[j\varphi(t)] \tag{13}$$

where $\varphi(t)$ is the phase of $a(t)$. One can then get the following relationship:

$$|b(t)| = |a(t)| \tag{14a}$$

$$f(t) = \frac{\varphi(t)}{m\Omega}. \tag{14b}$$

Based on (8) and (14), we get the following expressions to design the filter. The coefficients and time delays are given by

$$\tau_k + \frac{\varphi(\tau_k)}{m\Omega} = kT \tag{15a}$$

$$\beta_k = \left| \frac{a(\tau_k)}{1 + \varphi'(\tau_k)/m\Omega} \right|. \tag{15b}$$

As a conclusion, to realize the desired bandpass response, if a regular FIR filter is used, the tap coefficients are determined

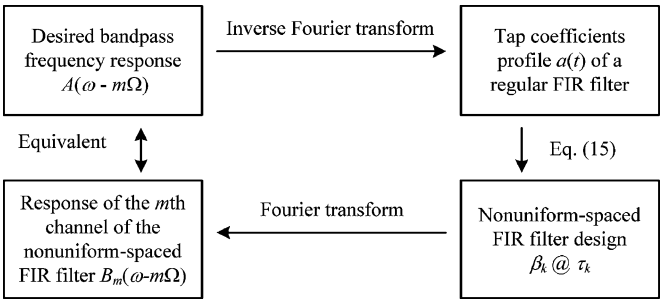

Fig. 2. Design procedure of a nonuniformly spaced FIR filter.

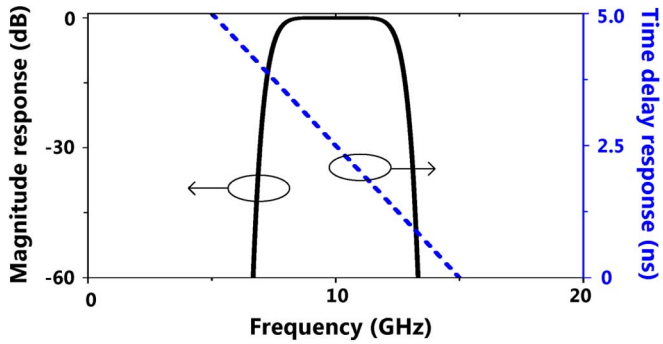

Fig. 3. Frequency response of the bandpass of interest. Solid line: the desired magnitude response. Dotted line: the desired time-delay response.

by (3), which may be negative or complex valued; however, if a nonuniformly spaced FIR filter is used, the tap coefficients and time delays are determined by (15) and the filter has positive-only coefficients.

The above analysis provides a way to implement a FIR filter with all-positive coefficients, but having an arbitrary bandpass response. The design process involves four steps, which is illustrated in Fig. 2.

III. Filter Design

As an example, a bandpass filter with a flat-top and a quadratic phase response is designed and analyzed. We assume that the frequency response of the passband is located at $f_0 = 10$ GHz, with a full-width at half-width (FWHM) of 5 GHz, as shown in Fig. 3. The desired magnitude response has a shape of a fourth-order super Gaussian. Since the desired phase response is quadratic, the corresponding time-delay response is then a linear function of frequency f, which is given by $\tau(f) = -50T \times (f - f_0)$, where $T = 100$ ps is a uniform time-delay difference.

If the filter is a regular FIR filter with uniformly spaced taps, the filter can be designed based on (3). After the inverse Fourier transform, we have the design of the regular FIR filter, with the tap coefficients plotted in Fig. 4.

As can be seen, complex tap coefficients are required. The frequency response of the FIR filter can be calculated by the Fourier transform, which is given by

$$H(\omega) = \sum_k \alpha_k \exp(-jkT\omega). \tag{16}$$

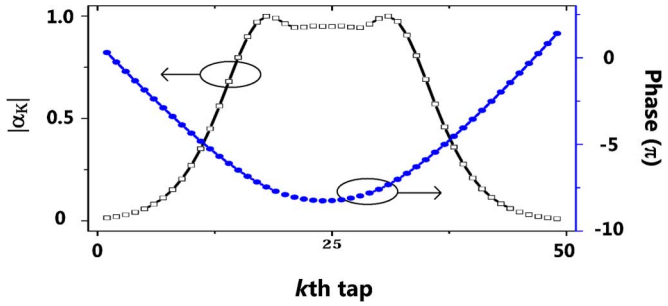

Fig. 4. Design of a regular FIR design. □ line: absolute value of the tap coefficients. • line: phase of the coefficients.

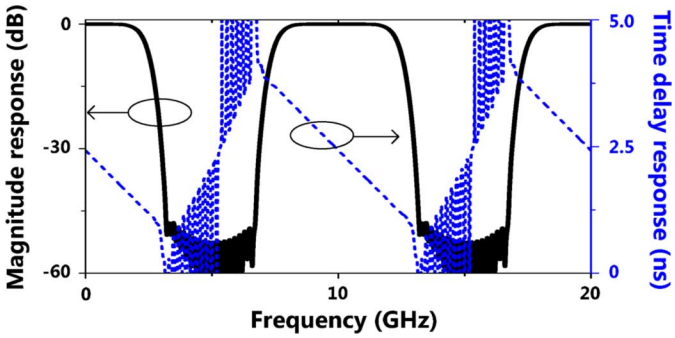

Fig. 5. Frequency response of the regular FIR filter. Solid line: magnitude response. Dotted line: time delay response.

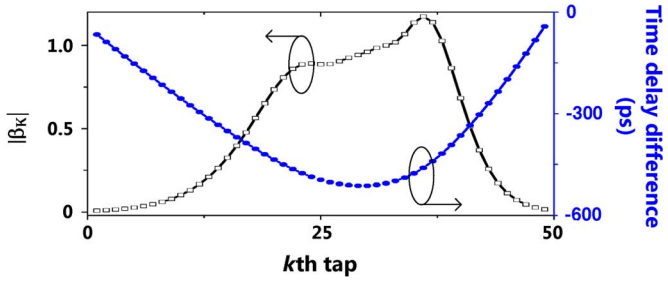

Fig. 6. Design of a nonuniformly spaced FIR filter. □ line: the value of the tap coefficients. • line: the time-delay difference of each tap.

Fig. 5 shows the calculation result, where the desired bandpass response is realized.

We apply the proposed technique to design the filter with all-positive coefficients to realize the same bandpass response by nonuniform sampling. The design is made based on the procedure illustrated in Fig. 2. Based on (15), the tap coefficients and the time-delay differences are calculated and plotted in Fig. 6, where the time delay difference is defined as

$$\Delta\tau_k = \tau_k - kT. \tag{17}$$

Theoretically, m could be any nonzero value. In this example, $m = 1$ is selected. As can be seen, the tap coefficients are positive only, and the time-delay spacing is nonuniform. The frequency response is calculated by the Fourier transform

$$\tilde{H}(\omega) = \sum_k \beta_k \exp(-j\tau_k\omega) \tag{18}$$

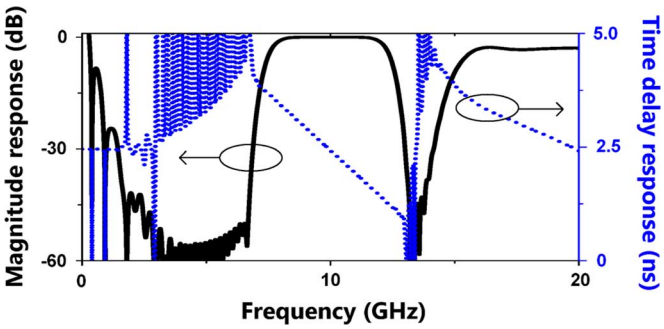

Fig. 7. Spectral response of the nonuniformly spaced FIR filter. Solid line: magnitude response. Dotted line: time-delay response.

which is shown in Fig. 7. Clearly, the desired magnitude and phase responses are realized in the first-order channel of the spectral response of the nonuniformly spaced FIR filter. Comparing the response in Fig. 7 with that shown in Fig. 5, one can see that an identical frequency response, both in magnitude and phase, is obtained, which confirms the effectiveness of the proposed technique to design a FIR filter with all positive coefficients through nonuniform sampling, as discussed in Section II.

It is different from a regular FIR filter in which the spectral responses at different channels are identical; a nonuniformly spaced FIR filter has different frequency responses at different channels, which can be seen from (11). The difference is resulted from the fact that equivalent phase shifts introduced to the tap coefficients are different for different channels, i.e., the equivalent phase shift corresponding to the mth channel is $m\Omega f(t)$. Fig. 8 shows the multichannel frequency response of the nonuniformly spaced FIR filter corresponding to the design in Fig. 6, and the regular filter corresponding to the design in Fig. 4. Obviously, the frequency responses of all channels of the regular FIR filter are identical. Once the FSR of the filter is larger than the bandwidth of $A(\omega)$, all the channels will be well separated. However, the frequency responses of the channels of the nonuniformly spaced FIR filter are different. As can be seen the tap coefficients will experience larger phase shifts for a higher order channel, leading to an increased bandwidth, as shown in Fig. 8(a). If the channel bandwidth is larger than the FSR, the adjacent channels will then interfere, generating large ripples between the channels, as also shown in Fig. 8(a). The adjacent channel interference must be avoided in the filter design. For practice applications, the channel of interest should be well separated from its adjacent spectral channels, giving an upper limit of the relative bandwidth of the filter when the mth-order channel is used, which is $1/m$.

It should also be noted that when $m = 0$, there are no equivalent phase shifts introduced to the tap coefficients, as can be seen from (10), as well as the simulation result shown in Fig. 8(a). As a result, the filter will always have a resonance at the baseband. For many applications, the baseband resonance should be eliminated. A solution to eliminate the baseband resonance is to use a phase modulator in the FIR filter. It has been demonstrated [20] that PM to intensity modulation (IM) conversion in a dispersive element would generate a notch at dc, which would be used to eliminate the baseband resonance of a nonuniformly spaced FIR filter. The filter setup using a phase modulator is illustrated in

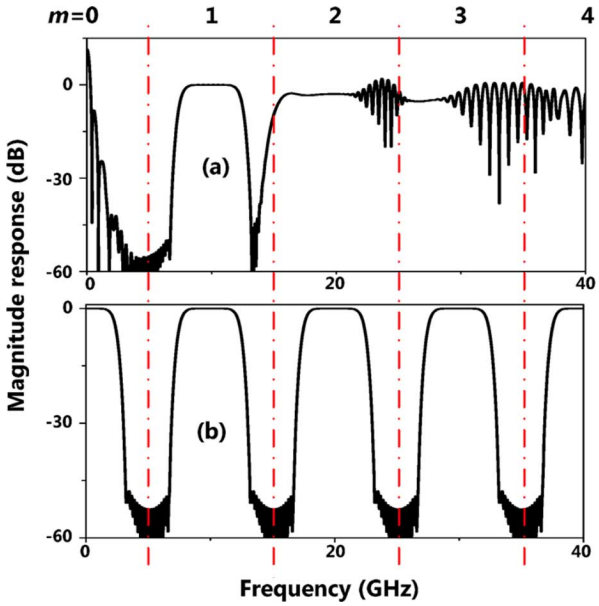

Fig. 8. Multichannel frequency response of a: (a) nonuniformly spaced FIR filter and (b) regular FIR filter. The first four channels are plotted.

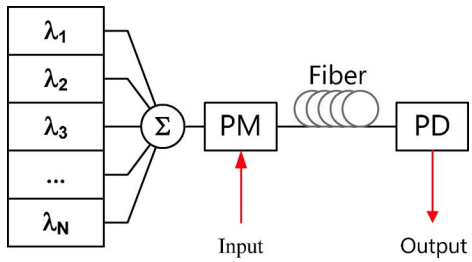

Fig. 9. Realization of the nonuniformly spaced FIR filter. The baseband resonance is eliminated by the notch at dc due to the PM-IM conversion. Phase modulator: PM. Photodetector: PD.

Fig. 9. The dispersive element in the setup is a length of dispersive fiber such as dispersion compensating fiber or standard single-mode fiber.

As discussed in [20], the PM-IM conversion in a dispersive element would lead to a transfer function given by

$$H_{\text{PM-IM}}(\omega) = \cos\left(\frac{\chi\lambda^2\omega^2}{4\pi c} + \frac{\pi}{2}\right) \tag{19}$$

where c is the light velocity in free space, $\chi = DL$ is the total dispersion of the dispersive device, D is the dispersion coefficient, L is the length of the dispersive fiber, and λ is the central wavelength of the optical carrier. Clearly, the transfer function has a notch as dc. By properly selecting the total dispersion, the first peak of the transfer function $H_{\text{PM-IM}}(\omega)$ can be designed to locate at the same location as the channel of interest. If $m = 1$ is selected and the first peak of $H_{\text{PM-IM}}(\omega)$ is located at the first-order channel of the filter, then we can calculate the required dispersion by the following equation:

$$\chi = \frac{2\pi^2 c}{\lambda^2\Omega^2}. \tag{20}$$

For example, to implement a FIR filter with a flat top and quadratic phase response, as studied in Section III, the required

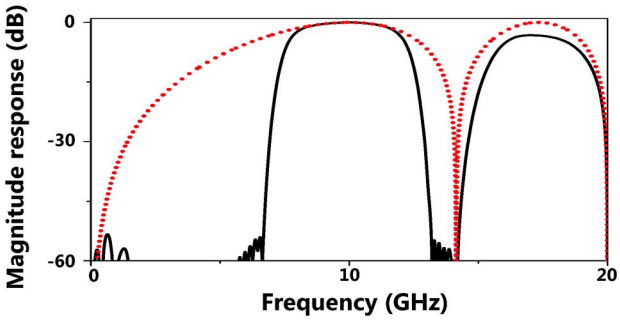

Fig. 10. Frequency response of the nonuniformly spaced FIR filter implemented using a phase modulator. Dotted line: frequency response of the PM-IM conversion. Solid line: total frequency response of the filter.

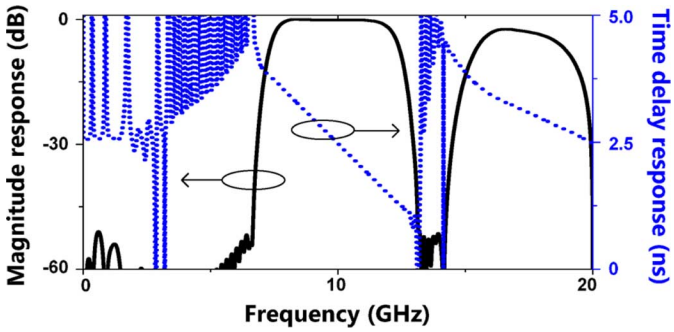

Fig. 12. Frequency response of the FIR filter incorporating the frequency response of the PM-IM conversion.

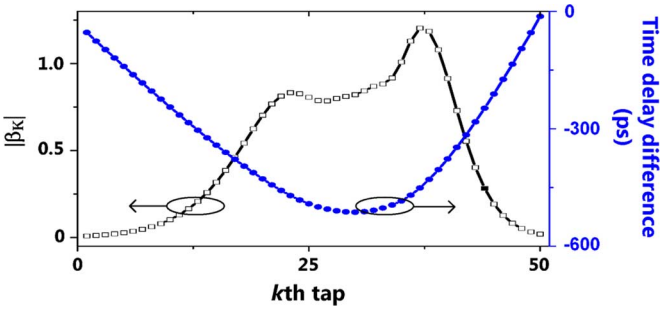

Fig. 11. New FIR filter design considering the PM-IM conversion.

dispersion calculated based on (20) is 624.3 ps/nm, corresponding to the dispersion of a standard single-mode fiber with a length of about 36.7 km. The total frequency response of the filter incorporating the frequency response of the PM-IM conversion is shown in Fig. 10. It should be noted, however, that the frequency response of the PM-IM conversion is not flat. If the desired bandpass response has a large bandwidth, $H_{\text{PM-IM}}(\omega)$ will add an additional magnitude response to the bandpass concerned, making the total frequency response nonflat.

To compensate for the additional magnitude response due to PM-IM conversion, the response of the PM-IM conversion must be considered during the design of the nonuniformly spaced FIR filter, i.e., the original target response, $A(\omega - m\Omega)$, should be replaced by $(A(\omega - m\Omega)/(H_{\text{PM-IM}}(\omega))$. With the above consideration, a new FIR filter is designed, with the tap coefficients and time-delay differences shown in Fig. 11.

Based on (18) and (19), the frequency response of the new filter is calculated, which is shown in Fig. 12. Clearly, the baseband resonance is eliminated; meanwhile the nonflatness due to the PM-IM conversion is also well compensated by the inclusion of the spectral response of the PM-IM conversion in the design.

The filter discussed above has 50 taps. To implement the filter, a laser array with 50 wavelengths is required, which is not available in the laboratory. To proof the concept, we implement a nonuniformly spaced FIR filter with seven taps [17]. The filter is designed to have a passband response with a flat top and zero chirp (or a linear phase response) via nonuniform sampling. The procedure shown in Fig. 2 is used to perform the design. In the design, $m = 1$ is selected with a central frequency of 12.1 GHz and a 3-dB relative bandwidth of 0.4. The nonflat frequency response of the PM-IM conversion is also incorporated in the design. The parameters of the designed filter are given as follows: the tap coefficients are $[0.12, 0, 0.64, 1, 0.64, 0, 0.12]$ and the corresponding time delays are $[-2.5T, -2T, -T, 0, T, 2T, 2.5T]$, where T is equal to 85 ps. Clearly, the filter has all-positive coefficients with nonuniformly spaced taps.

The experimental setup to realize the seven-tap filter is shown in Fig. 9. Since two tap coefficients are zero, a laser array with five wavelengths is used. The time delays for different taps are achieved due to the chromatic dispersion of the dispersive fiber. To achieve the nonuniform spacing, the wavelengths are tuned to be nonuniformly spaced. Specifically, the wavelengths of the laser array are given by

$$\lambda_k = \lambda_0 + \frac{\tau_k - \tau_0}{\chi} \tag{21}$$

where λ_0 is the wavelength for the zeroth tap. In the experiment, 25-km standard single-mode fiber is used as the dispersive fiber with a total dispersion of about 425 ps/nm, and $\lambda_0 = 1543.3$ nm. Therefore, the wavelengths are $[1542.8, 1543.1, 1543.3, 1543.5, 1543.8]$ nm. The desired coefficients are obtained by controlling the output powers at the different wavelengths.

The frequency response of the filter is then measured using a vector network analyzer (VNA, Agilent E8364A), which is shown in Fig. 13. As can be seen the center frequency of the frequency response is located at 12.1 GHz with a flat top. The 3-dB bandwidth is about 5 GHz or a relative bandwidth about 0.42. The constant group-delay response measured in the experiment shows that the filter is chirp free. Based on the results, we conclude that a FIR filter having a bandpass response with flat top and zero chirp is realized by a positive-coefficient-only FIR filter via nonuniform sampling. Due to the unavailability of a laser array with 50 wavelengths at the time of experiment, the implementation was done with a laser array with only five wavelengths. However, the theoretically designed and the experimentally realized filter share the same principle and the same setup, as shown in Fig. 9. The complexity of the filter when employing a large number of laser sources will not increase significantly. This is very different from other schemes for the implementation a filter with complex coefficients. For example, for a filter with complex coefficients based on the SBS, in addition to the

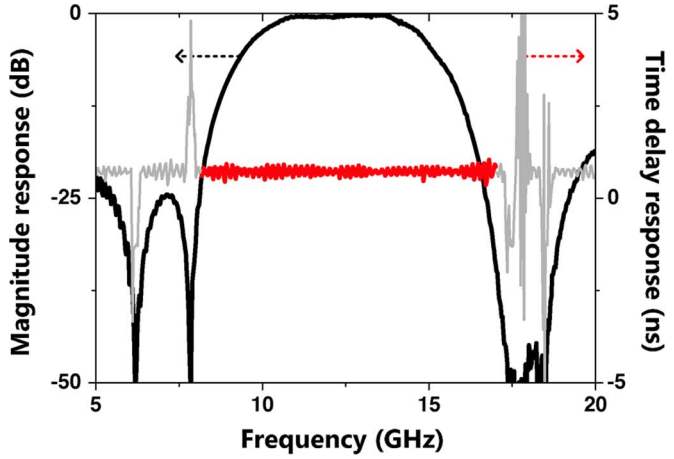

Fig. 13. Measured frequency response of the flat-top chirp-free photonic microwave filter based on nonuniformly spaced sampling. The time delay response within the 3-dB bandwidth is highlighted in red (in online version), which is constant with the bandwidth.

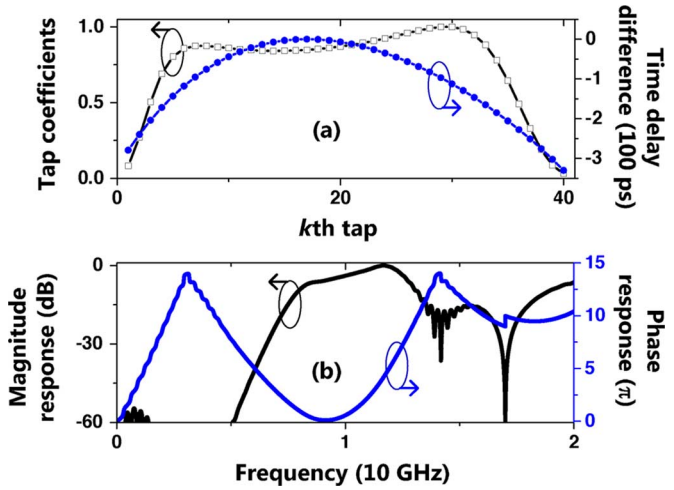

Fig. 14. (a) Filter design for the chirped pulse generation. □ line: tap coefficient profile. • line: time-delay different. (b) Spectral response of the filter. Both the magnitude and phase responses are shown.

same requirement for a large number of laser sources, a large number of nonlinear fibers and pump sources are also required, which makes the complexity of the filter significantly increased.

IV. Applications in Micorwave Signal Processing

In addition to signal filtering in which the filters are mostly designed to have a flat top and chirp free, the proposed technique is particularly useful for advanced signal processing, such as chirped or phase-coded signal generation, and microwave matched filtering.

Microwave pulses with a large time bandwidth product (TBWP) are widely used in modern radar, computed tomography, and spread-spectrum communications systems [21], [22]. To achieve a large TBWP, the pulses are usually frequency chirped or phase coded. The generation of such pulses in the optical domain has the advantage of high speed and broad bandwidth. Photonic approaches proposed recently include direct space-to-time optical pulse shaping [23], [24], and wavelength-to-time mapping [25], [26]. A general way to generate an arbitrary microwave pulse is to shape the spectrum of a short microwave pulse, to make the spectrum of the shaped pulse identical to what we expect to generate. The spectrum shaping can be done using a microwave filter. Assume the spectra of the input pulse and the output pulse are, respectively, $X(\omega)$ and $Y(\omega)$, the microwave filter should have a spectral response given by

$$H(\omega) = \frac{Y(\omega)}{X(\omega)}. \tag{22}$$

Since the desired pulse usually has complicated phase response, the filter to generate the required spectral response should have negative or complex tap coefficients. It should be noted that the desired microwave pulse with a large TBWP has usually a relative bandwidth less than 1. As a result, the required spectral response can then be achieved by the proposed technique to use a nonuniformly spaced photonic microwave FIR filter with all-positive coefficients.

A. Chirped Microwave Pulse Generation [18]

A chirped microwave pulse can be generated by passing a broadband chirp-free microwave pulse through a microwave filter with a quadratic phase response or a linear group-delay response. The design of a FIR filter with a quadratic phase response has been described in Section III. However, to ensure that the generated chirped pulse has a flat temporal envelope, the spectrum of the input pulse has to be considered based on (22). In the following, a design example is provided. Mathematically, the desired chirped pulse is expressed as

$$y(t) = \exp\left[-\ln(2)\left(\frac{2t}{W}\right)^8\right] \times \exp\left[j\left(\frac{2\pi}{T}t + \pi\gamma t^2\right)\right] \tag{23}$$

where $W = 3.2$ ns is the FWHM, $T = 100$ ps is the mean period, and $\gamma = 1.6$ GHz/ns is the chirp rate. The setup to implement the generation is shown in Fig. 9.

A length of 25-km standard single-mode fiber with total dispersion of $\chi = 425$ ps/nm is used. If we assume the chirped microwave pulse is generated from a chirp-free Gaussian pulse with an FWHM of 60 ps, the required filter response is calculated from (22), and the corresponding design is then calculated following the procedure given in Section III. The filter has 40 taps and the tap coefficients and the time delays are shown in Fig. 14(a) and the frequency response of the filter is shown in Fig. 14(b). As can be seen, the filter has a bandpass response with a central frequency at around 10 GHz and the phase response in the passband is quadratic. Again, the baseband resonance is eliminated the PM-IM conversion in a dispersive fiber.

If a Gaussian pulse with an FWHM of 60 ps is sent to the filter, the output pulse would be chirped. The spectrum of the generated chirped pulse and its temporal waveform are calculated and plotted in Fig. 15(a) and (b). The chirp rate is 1.6 GHz/ns, which is equal to the desired value.

The generation of a chirped microwave pulse using a five-tap nonuniformly spaced microwave FIR filter is then experimentally demonstrated. The desired pulse has an FWHM of 550 ps,

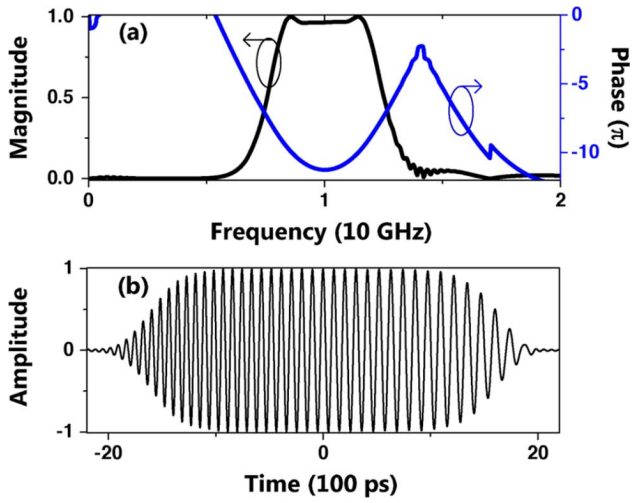

Fig. 15. (a) Spectrum of the chirped RF pulse. (b) Temporal shape of the pulse.

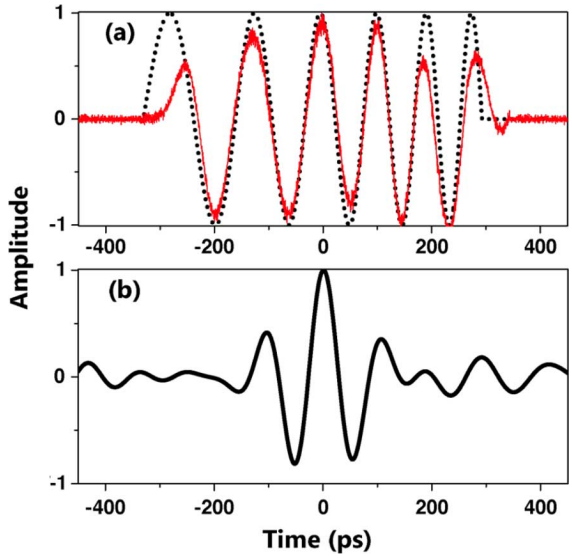

Fig. 16. (a) Solid line: generated chirped RF pulse. Dotted line: desired chirped RF pulse. (b) Correlation between the measured and reference pulses.

a mean period of 110 ps, and a chirp rate of 13.2 GHz/ns, as shown via the dotted line in Fig. 16(a). The input pulse is a chirp-free Gaussian pulse generated in the experiment by a pattern generator with an FWHM of 65 ps. The five-tap FIR filter is designed based on the procedure in Section III. The time delays of the taps are $T \times [-2.31, -1.08, 0.00, 0.81, 1.51]$, where $T = 110$ ps. The wavelengths from the multiwavelength source are then calculated based on (21). In our experiment, λ_0 is 1543.30 nm, and the five wavelengths are set as $[1542.70, 1543.02, 1543.30, 1543.51, 1543.69]$ nm. In the experiment, the output power of each laser is controlled such that the tap coefficients α_k are optimized to minimize the error between the desired and the generated chirped pulses. The tap coefficients are calculated to be $[1.0, 1.0, 1.0, 1.5, 1.4]$. Again, the setup shown in Fig. 9 is used to perform the chirped pulse generation. The dispersive fiber is a length of 25-km standard single-mode fiber with a total dispersion of about 425 ps/nm. The generated pulse is then measured by a high-speed oscilloscope (Agilent 86100C), which is shown as the solid line in Fig. 16(a). Obviously, a chirped RF pulse having a shape close to the theoretical microwave chirped pulse is generated. A slight distortion in the pulse shape is due to the small tap number. It is known that a chirped pulse can be compressed at a receiver using a matched filter. To demonstrate the pulse compression performance, we calculate the correlation between the measured and reference chirped microwave pulses [the two curves in Fig. 16(a)], and the result is shown in Fig. 16(b). It is clearly seen that the microwave pulse is compressed, which confirms that the generated microwave pulse is chirped.

B. Phase Coded Microwave Pulse Generation [16]

Similar to a chirped microwave pulse, a phase coded microwave pulse can also be generated using a nonuniformly spaced FIR filter, which can find many applications such as in radar and communications systems. The fundamental principle is to introduce the phase information to the generated pulse by time delays, as shown in Fig. 17.

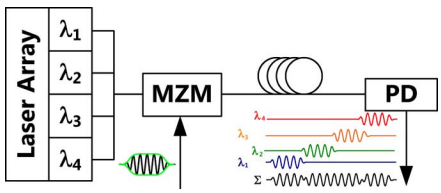

Fig. 17. Proposed photonic microwave FIR filter for microwave phase coding.

Obviously, the tap number of the FIR filter should be the same as the chip number of the desired phase-coded signal. In a regular microwave FIR filter, the time-delay differences between adjacent taps are identical as T. As we discussed in Section II, the frequency response of a FIR filter is periodic with the kth spectral channel located at $\omega = 2k\pi/T$. If there are m microwave cycles in each chip, then $m = T/T_0 = T\omega/2\pi$ or $\omega = 2m\pi/T$, where T_0 is the period of the microwave carrier, we then have $k = m$, which means that, for a chip that contains m microwave cycles, the filter frequency response concerned is located at the mth spectral peak. To implement the phase coding using a FIR filter, the phase of the kth chip should be introduced by the filter with the same phase φ_k at the kth tap. For example, to generate a phase-coded pulse with a code pattern of $\{0, \pi, \pi, 0\}$, the tap number N should be 4 and φ_k should be $\{0, \pi, \pi, 0\}$. Therefore, a FIR filter with both positive and negative coefficients of $\{1, -1, -1, 1\}$ is required if a regular microwave FIR filter is used. In addition, if the phase code has arbitrary phase shifts, a microwave FIR filter with complex coefficients is required.

To generate the required phase code using a FIR filter with all positive coefficients, a FIR filter with nonuniformly spaced taps should be employed. The desired phase coding is implemented by adjusting the time-delay differences between the adjacent taps. According to (15a), we have

$$\tau_k = T \times \left(k - \frac{\varphi_k}{2\pi m}\right) = \left(km - \frac{\varphi_k}{2\pi}\right) T_0, \qquad k = 0, 1, 2, \ldots, N-1. \quad (24)$$

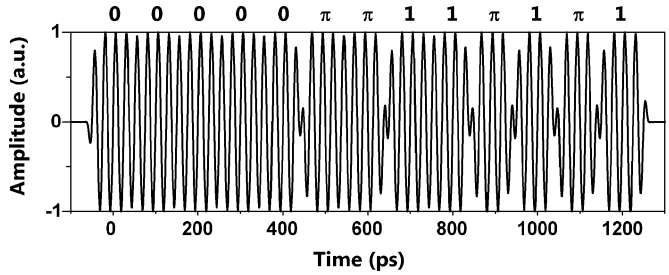

Fig. 18. Phase-coded microwave pulse with a 13-chip Barker code generated by a nonuniformly spaced FIR filter.

TABLE I
FOUR SETS OF WAVELENGTHS FOR FOUR DIFFERENT CODE PATTERNS

Code pattern	Wavelength set (nm)			
{0,0,0,0}	1543.184	1543.984	1544.784	1545.584
{0,π,π,0}	1543.184	1543.884	1544.684	1545.584
{0,π,0,π }	1543.184	1543.884	1544.784	1545.484
{0,π/2,π,3π/2}	1543.184	1543.934	1544.684	1545.434

For example, for a four-tap filter, we have $N = 4$. If $m = 4$ is selected, for a code pattern of $\{0, \pi, \pi, 0\}$ the time delays should be $\{0, 7/8T, 15/8T, 3T\}$.

As a design example, a binary phase coded microwave signal with a 13-chip Barker code, $[+1, +1, +1, +1, +1, -1, -1, +1, +1, -1, +1, -1, +1]$, is generated. The Barker codes are usually used in direct-sequence spread-spectrum communications systems and pulse compression radar systems thanks to the excellent correlation performance [27]. In the design, the carrier frequency is 40 GHz and $m = 4$, i.e., the chip rate is 10 GHz, and t_0 is 25 ps. Based on (24), the time delays of all the taps are calculated, which are given $[0, 4, 8, 12, 16, 19.5, 23.5, 28, 32, 35.5, 40, 43.5, 48] \times 25$ ps. If the input microwave signal is a super-Gaussian pulse with an FWHM of 100 ps, the output of the filter is calculated, which is shown in Fig. 18. The desired phase coding is realized.

A four-tap microwave delay-line filter with adjustable time-delay differences to generate tunable phase code patterns based on the experimental setup shown in Fig. 17 is demonstrated. In the experiment, the input microwave signal is a super-Gaussian pulse with a carrier frequency of 5.94 GHz and an FWHM of about 680 ps. The single-mode fiber in our experiment has a length of about 50 km. The wavelength of each tunable laser source is calculated based on (24) and (21). Four code patterns are generated in our experiment. The wavelengths for the generation of the four code patterns are listed in Table I. Note that λ_0 is 1543.184 nm. When the wavelengths of the tunable laser sources are tuned at one of the four sets of wavelengths in the table, a microwave pulse with the phase code pattern corresponding to the specific set of wavelengths is obtained at the output of the PD. The generated pulse is monitored by a high-speed oscilloscope and is shown in Fig. 19.

C. Microwave Matched Filtering [19]

In a radar or communications system, if a transmitted signal is chirped or phase coded, at the receiver end a matched filter should then be used to detect the presence of the chirped or phase-coded signal. Although the decoding process can be done using an electronic matched filter, the processing speed is limited due to the low sampling rate of the currently available digital electronics. A solution to the problem is to perform matched filtering in the optical domain. It is known that a decoding process is actually to calculate the correlation between the received microwave signal and the reference signal. A correlator or matched filter should have a spectral response that is a complex-conjugated version of the spectral response of the incoming microwave signal. Such a microwave correlation operation can obviously be implemented by a photonic microwave FIR filter.

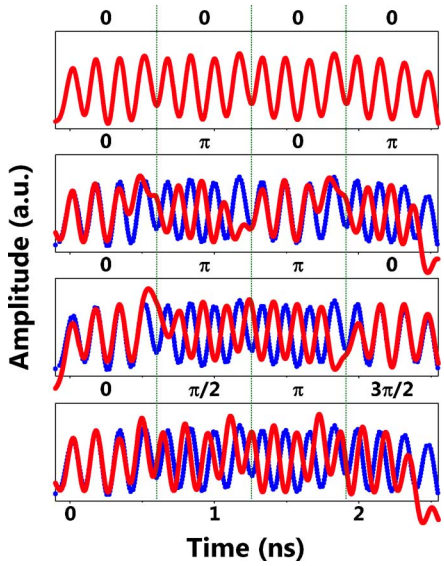

Fig. 19. Experimentally generated phase-coded microwave pulses (red solid line in online version). Blue dotted line (in online version): microwave signals without phase coding.

Assume that a phase-coded microwave signal is express as $W(t)\cos[\omega t + \varphi(t)]$, where ω is the angular frequency of the microwave carrier, $\varphi(t)$ is the phase coding function, and $W(t)$ is a rectangle window function, which is constant for $-p/2 \leqslant t < p/2$, while 0 otherwise. At the receiver, the correlation between the phase-coded signal and a reference microwave signal, $W(t)\cos[\omega t + \theta(t)]$, is calculated. If the correlator is matched to the signal, then $\theta(t) = \varphi(t)$, an auto-correlation with a large correlation peak is achieved and the signal will be detected; otherwise, $\theta(t)$ is orthogonal to $\varphi(t)$, then we get a cross-correlation and a low correlation peak would be generated at the receiver. In the both cases, the output from the receiver should be

$$R(t) = W(t)\cos[\omega t + \varphi(t)] * W(-t)\cos[-\omega t + \theta(-t)] \tag{25}$$

where * denotes convolution operation. If the above correlation is performed by a microwave FIR filter, then based on (25) such a filter should have an impulse response given by

$$h(t) = \frac{1}{2}W(-t)\exp[j\omega t - j\theta(-t)] + c.c. \tag{26}$$

To realize the filter in (26), a FIR filter can be used. Based on signal processing theory, a FIR filter can be implemented

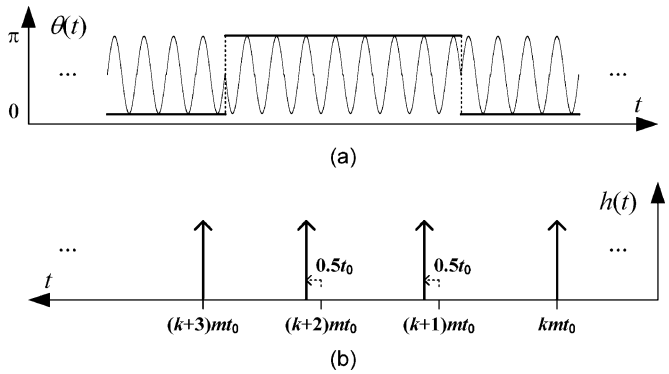

Fig. 20. (a) Phase characteristic of the RF signal. The bi-phase coding is taken as example. (b) Corresponding nonuniform spacing FIR filter structure.

through sampling the input signal with a uniform spacing. If the sampling period is $T = 2m\pi/\omega = mT_0$, where m is an integer and T_0 is the period of the microwave carrier, then the impulse response in (26) can be obtained in the mth-order channel of the FIR filter. Since the impulse response has a nonzero PM, the FIR filter has multiple complex taps, i.e., the phase of the kth tap should be $-\theta(-kT)$.

The filter can be designed to have equivalent complex coefficients using an all-positive-coefficient FIR filter based on the nonuniform sampling. Based on (15b), the time delays of the filter are calculated by

$$\tau_k = kT + \frac{\theta(-\tau_k)}{2m\pi}T = \left[km + \frac{\theta(-\tau_k)}{2\pi}\right]T_0. \qquad (27)$$

The frequency response of the filter expressed in (26) is then realized in the mth channel of the frequency response of the new filter.

Assume that a phase coded signal has N chips, and each chip has m cycles of the RF carrier. Based on (27), the filter time delays of the filter are then calculated by

$$\tau_k = \left(km + \frac{\theta_{N+1-k}}{2\pi}\right)T_0 \qquad (28)$$

where θ_k is the phase of the kth tap, $1 \leqslant k \leqslant N$. The structure of the nonuniform sampling FIR filter is illustrated in Fig. 20.

For the phase-coded signal shown in Fig. 18, a nonuniformly spaced FIR filter to perform the matched filtering is designed. Based on (28), and considering that the phase code is a 13-chip Barker code, the time delays of all the taps are calculated, which are $[0, 3.5, 8, 11.5, 16, 20, 23.5, 27.5, 32, 36, 40, 44, 48] \times 25$ ps. When the phase-coded signal in Fig. 18 is sent to the matched filter, a correlation output is obtained, as shown in Fig. 21. Clearly, the signal is successfully decoded.

To proof the concept, a photonic microwave FIR filter to decode the four-chip binary phase-coded microwave signal is experimentally demonstrated. Again, the system setup shown in Fig. 9 is used. The dispersive fiber is a 25-km single-mode fiber. The output is measured by a high-speed oscilloscope (Agilent 86100C). The input signal has a 6.75-GHz carrier which is phase coded by a four-chip Barker code, $[+1, -1, +1, +1]$. In our design, $m = 4$ so that the chip rate is 1.6875 GHz. Based on (28), the time delays for the four taps are then calculated, which are given $[0.5926, 1.1852, 1.8519, 2.3704]$ ns. The wavelengths

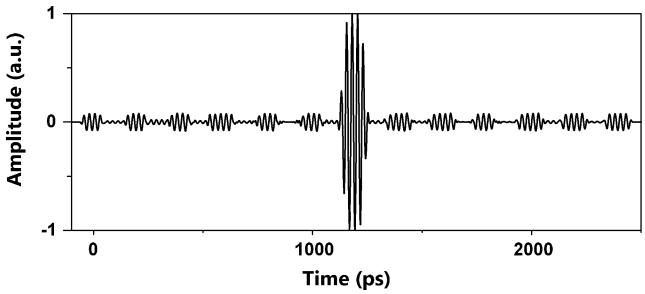

Fig. 21. Correlation at the output of the nonuniformly spaced FIR matched filter.

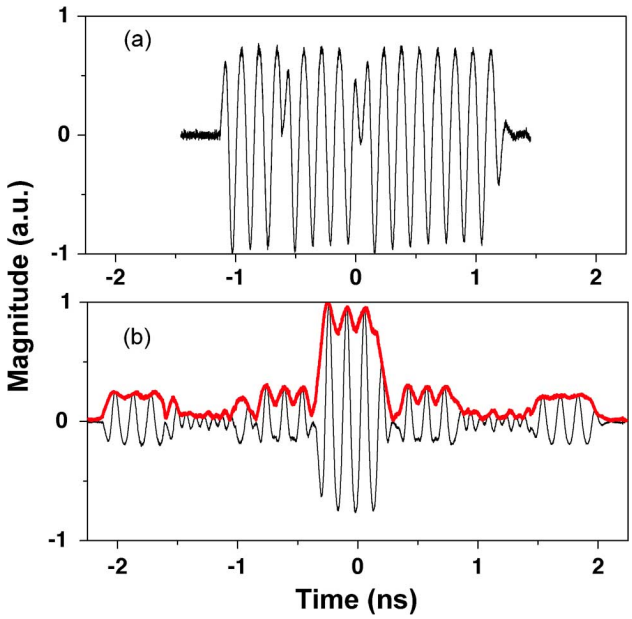

Fig. 22. (a) Input phase-coded microwave signal. (b) Measured correlation output (black solid line) with the calculated absolute envelope (red solid line in online version).

of the four lasers are then calculated according to (21), which are given $[1543.10, 1544.49, 1546.06, 1547.28]$ nm. The original input phase coded microwave signal is shown in Fig. 22(a). When the phase-coded signal is sent to the nonuniformly spaced FIR filter, an auto-correlation is obtained at the output of the filter, which is shown in Fig. 22(b). It is clearly seen that the phase-coded signal is correctly decoded.

V. Conclusion

An overview of the design and implementation of photonic microwave FIR filters with nonuniform sampling was performed. We have shown that a microwave FIR filter with all positive coefficients can be implemented to generate arbitrary bandpass response through nonuniform sampling. Based on the analysis, a 50-tap bandpass filter with a flat top and a quadratic phase response was designed and analyzed. A seven-tap nonuniformly spaced photonic microwave filter with a flat top and chirp-free bandpass response was experimentally demonstrated. The key significance of the technique is that a nonuniformly spaced FIR filter can be used to perform advanced microwave signal processing. In this paper, the applications of the technique for microwave signal processing, including

the generation of chirped and phase-coded microwave pulses, and the implementation of matched filtering, were discussed. Both theoretical designs and experimental demonstrations were provided.

REFERENCES

[1] J. Capmany, B. Ortega, and D. Pastor, "A tutorial on microwave photonic filters," *J. Lightw. Technol.*, vol. 24, no. 1, pp. 201–229, Jan. 2006.

[2] R. A. Minasian, "Photonic signal processing of microwave signals," *IEEE Trans. Microw. Theory Tech.*, vol. 54, no. 2, pp. 832–846, Feb. 2006.

[3] S. Sales, J. Capmany, J. Marti, and D. Pastor, "Experimental demonstration of fiber-optic delay line filters with negative coefficients," *Electron. Lett.*, vol. 31, no. 13, pp. 1095–1096, Jul. 1995.

[4] F. Coppinger, S. Yegnanarayanan, P. D. Trinh, and B. Jalali, "All-optical RF filter using amplitude inversion in a semiconductor optical amplifier," *IEEE Trans. Microw. Theory Tech.*, vol. 45, no. 8, pp. 1473–1477, Aug. 1997.

[5] Y. Yan, F. Zeng, Q. Wang, and J. P. Yao, "Photonic microwave filter with negative coefficients based on cross polarization modulation in a semiconductor optical amplifier," in *OFC 2007*, 2007, Paper OWU6.

[6] S. Li, K. S. Chiang, W. A. Gambling, Y. Liu, L. Zhang, and I. Bennion, "A novel tunable all-optical incoherent negative-tap fiber-optic transversal filter based on a DFB laser diode and fiber Bragg gratings," *IEEE Photon. Technol. Lett.*, vol. 12, no. 9, pp. 1207–1209, Sep. 2000.

[7] X. Wang and K. T. Chan, "Tunable all-optical incoherent bipolar delay-line filter using injection-locked Fabry–Pérot laser and fiber Bragg gratings," *Electron. Lett.*, vol. 36, no. 24, pp. 2001–2002, Dec. 2000.

[8] J. Mora, M. V. Andres, J. L. Cruz, B. Ortega, J. Capmany, D. Pastor, and S. Sales, "Tunable all-optical negative multitap microwave filters based on uniform fiber Bragg gratings," *Opt. Lett.*, vol. 28, no. 15, pp. 1308–1310, Aug. 2003.

[9] J. Capmany, D. Pastor, A. Martinez, B. Ortega, and S. Sales, "Microwave photonics filters with negative coefficients based on phase inversion in an electro-optic modulator," *Opt. Lett.*, vol. 28, no. 16, pp. 1415–1417, Aug. 2003.

[10] E. H. W. Chan and R. A. Minasian, "Novel all-optical RF notch filters with equivalent negative tap response," *IEEE Photon. Technol. Lett.*, vol. 16, no. 5, pp. 1370–1372, May 2004.

[11] F. Zeng and J. P. Yao, "All-optical bandpass microwave filter based on an electro-optical phase modulator," *Opt. Exp.*, vol. 12, no. 16, pp. 3814–3819, Aug. 2004.

[12] J. Wang, F. Zeng, and J. P. Yao, "All-optical microwave bandpass filters implemented in a radio-over-fiber link," *IEEE Photon. Technol. Lett.*, vol. 17, no. 8, pp. 1737–1739, Aug. 2005.

[13] N. You and R. A. Minasian, "A novel tunable microwave optical notch filter," *IEEE Trans. Microw. Theory Tech.*, vol. 49, no. 10, pp. 2002–2005, Oct. 2001.

[14] Y. Yan and J. P. Yao, "A tunable photonic microwave filter with a complex coefficient using an optical RF phase shifter," *IEEE Photon. Technol. Lett.*, vol. 19, no. 10, pp. 1472–1474, Oct. 2007.

[15] A. Loayssa, J. Capmany, M. Sagues, and J. Mora, "Demonstration of incoherent microwave photonic filters with all-optical complex coefficients," *IEEE Photon. Technol. Lett.*, vol. 18, no. 8, pp. 1744–1746, Aug. 2006.

[16] Y. Dai and J. P. Yao, "Microwave pulse phase encoding using a photonic microwave delay-line filter," *Opt. Lett.*, vol. 32, no. 24, pp. 3486–3488, Dec. 2007.

[17] Y. Dai and J. P. Yao, "Nonuniformly-spaced photonic microwave delay-line filter with improved bandpass characteristics," *Opt. Exp.*, vol. 16, no. 7, pp. 4713–4718, Mar. 2008.

[18] Y. Dai and J. Yao, "Chirped microwave pulse generation using a photonic microwave delay-line filter with a quadratic phase response," *IEEE Photon. Technol. Lett.*, vol. 21, no. 9, pp. 569–571, May 2009.

[19] Y. Dai and J. Yao, "Microwave correlator based on a nonuniformly spaced photonic microwave delay-line filter," *IEEE Photon. Technol. Lett.*, vol. 21, no. 14, pp. 969–971, Jul. 2009.

[20] F. Zeng and J. P. Yao, "Investigation of phase modulator based all-optical bandpass microwave filter," *J. Lightw. Technol.*, vol. 23, no. 4, pp. 1721–1728, Apr. 2005.

[21] A. W. Rihaczek, *Principles of High-Resolution Radar*. Norwood, MA: Artech House, 1996.

[22] M. Bertero, M. Miyakawa, P. Boccacci, F. Conte, K. Orikasa, and M. Furutani, "Image restoration in chirp pulse microwave CT (CP-MCT)," *IEEE Trans. Biomed. Eng.*, vol. 47, no. 5, pp. 690–699, May 2000.

[23] S. Xiao, J. D. McKinney, and A. M. Weiner, "Photonic microwave arbitrary waveform generation using a virtually-imaged phased-array (VIPA) direct space-to-time pulse shaper," *IEEE Photon. Technol. Lett.*, vol. 16, no. 8, pp. 1936–1938, Aug. 2004.

[24] J. D. McKinney, D. E. Leaird, and A. M. Weiner, "Millimeter-wave arbitrary waveform generation with a direct space-to-time pulse shaper," *Opt. Lett.*, vol. 27, no. 15, pp. 1345–1347, Aug. 2002.

[25] J. Chou, Y. Han, and B. Jalali, "Adaptive RF-photonic arbitrary waveform generator," *IEEE Photon. Technol. Lett.*, vol. 15, no. 4, pp. 581–583, Apr. 2003.

[26] C. Wang and J. P. Yao, "Photonic generation of chirped millimeter-wave pulses based on nonlinear frequency-to-time mapping in a nonlinearly chirped fiber Bragg grating," *IEEE Trans. Microw. Theory Tech.*, vol. 56, no. 2, pp. 542–553, Feb. 2008.

[27] N. Levanon and E. Mozeson, *Radar Signals*. Hoboken, NJ: Wiley, 2004.

Yitang Dai received the B.Sc. and Ph.D. degrees in electronic engineering from Tsinghua University, Beijing, China, in 2002 and 2006, respectively.

Since June 2007, he has been a Postdoctoral Research Fellow with the Microwave Photonics Research Laboratory, School of Information Technology and Engineering, University of Ottawa, Ottawa, ON, Canada. His research interests include fiber Bragg gratings (FBGs), optical CDMA, fiber lasers, microwave photonics, pulse shaping, semiconductor lasers, and optical sensors.

Jianping Yao (M'99–SM'01) received the Ph.D. degree in electrical engineering from the Université de Toulon, Toulon, France, in 1997.

In 2001, he joined the School of Information Technology and Engineering, University of Ottawa, Ottawa, ON, Canada, where he is currently a Professor, Director of the Microwave Photonics Research Laboratory, and Director of the Ottawa–Carleton Institute for Electrical and Computer Engineering. From 1999 to 2001, he held a faculty position with the School of Electrical and Electronic Engineering, Nanyang Technological University, Singapore. He holds a Yongqian Endowed Visiting Chair Professorship with Zhejiang University, Hangzhou, China. He spent three months as an invited professor in the Institut National Polytechnique de Grenoble, Grenoble, France, in 2005. He is an Associate Editor of the *International Journal of Microwave and Optical Technology*. He has authored or coauthored over 280 papers, including over 160 papers in peer-reviewed journals and 120 papers in conference proceeding. His research has focused on microwave photonics, which includes all-optical microwave signal processing, photonic generation of microwave, millimeter wave, and terahertz, radio-over-fiber, ultra-wideband (UWB) over fiber, FBGs for microwave photonics applications, and optically controlled phased-array antenna. His research interests also include fiber lasers, fiber-optic sensors, and bio-photonics.

Dr. Yao is a Registered Professional Engineer of Ontario, Canada. He is a Fellow of the Optical Society of America (OSA). He is a Senior Member of the IEEE Photonics Society and the IEEE Microwave Theory and Techniques Society (IEEE MTT-S). He is on the Editorial Board of the IEEE TRANSACTIONS ON MICROWAVE THEORY AND TECHNIQUES. He was the recipient of the 2005 International Creative Research Award of the University of Ottawa and the 2007 George S. Glinski Award for Excellence in Research. He was named University Research Chair in Microwave Photonics in 2007. He was a recipient of a Natural Sciences and Engineering Research Council of Canada (NSERC) Discovery Accelerator Supplements Award in 2008.